Published in final edited form as:
Magn Reson Imaging. 2013 November ; 31(9): . doi:10.1016/j.mri.2013.07.002.

Early assessment of breast cancer response to neoadjuvant chemotherapy by semi-quantitative analysis of high-temporal resolution DCE-MRI: Preliminary results

Richard G. Abramson[a,b,c,*], **Xia Li**[a,b], **Tamarya Lea Hoyt**[a,c], **Pei-Fang Su**[d], **Lori R. Arlinghaus**[a,b], **Kevin J. Wilson**[a,b], **Vandana G. Abramson**[c,e], **A. Bapsi Chakravarthy**[c,f], and **Thomas E. Yankeelov**[a,b,c,g,h,i]

[a]Department of Radiology and Radiological Sciences, Vanderbilt University, Nashville, TN

[b]Institute of Imaging Science, Vanderbilt University, Nashville, TN

[c]Vanderbilt-Ingram Center, Vanderbilt University, Nashville, TN

[d]Department of Statistics, National Cheng Kung University, Taiwan

[e]Department of Medicine, Vanderbilt University, Nashville, TN

[f]Department of Radiation Oncology, Vanderbilt University, Nashville, TN

[g]Department of Cancer Biology, Vanderbilt University, Nashville, TN

[h]Department of Biomedical Engineering, Vanderbilt University, Nashville, TN

[i]Department of Physics and Astronomy, Vanderbilt University, Nashville, TN

Abstract

Purpose—To evaluate whether semi-quantitative analysis of high temporal resolution dynamic contrast-enhanced MRI (DCE-MRI) acquired early in treatment can predict the response of locally advanced breast cancer (LABC) to neoadjuvant chemotherapy (NAC).

Materials and Methods—As part of an IRB-approved prospective study, 21 patients with LABC provided informed consent and underwent high temporal resolution 3 T DCE-MRI before and after 1 cycle of NAC. Using measurements performed by two radiologists, the following parameters were extracted for lesions at both examinations: lesion size (short and long axes, in both early and late phases of enhancement), radiologist's subjective assessment of lesion enhancement, and percentages of voxels within the lesion demonstrating progressive, plateau, or washout kinetics. The latter data were calculated using two filters, one selecting for voxels enhancing ≥50% over baseline and one for voxels enhancing ≥100% over baseline. Pretreatment imaging parameters and parameter changes following cycle 1 of NAC were evaluated for their ability to discriminate patients with an eventual pathological complete response (pCR).

Results—All 21 patients completed NAC followed by surgery, with 9 patients achieving a pCR. No pretreatment imaging parameters were predictive of pCR. However, change after cycle 1 of NAC in percentage of voxels demonstrating washout kinetics with a 100% enhancement filter discriminated patients with an eventual pCR with an area under the receiver operating characteristic curve (AUC) of 0.77. Changes in other parameters, including lesion size, did not predict pCR.

[*]Corresponding author. Vanderbilt University Medical Center, Department of Radiology and Radiological Sciences, 1161 21st Ave South, CCC-1121 MCN, Nashville, TN 37232-2675. richard.abramson@vanderbilt.edu. .

Conclusion—Semi-quantitative analysis of high temporal resolution DCE-MRI in patients with LABC can discriminate patients with an eventual pCR after one cycle of NAC.

Keywords

Response assessment; Preoperative chemotherapy; Primary chemotherapy; Imaging biomarkers; Operable breast cancer; DCE-MRI; Neoadjuvant therapy; Neoadjuvant chemotherapy; Enhancement kinetics

1. Introduction

Neoadjuvant chemotherapy (NAC) is offered to selected patients with locally advanced breast cancer (LABC) to reduce tumor burden before surgery and to allow for possible earlier treatment of occult micrometastatic disease [1]. Studies have confirmed that patients undergoing NAC have a lower risk of requiring mastectomy (i.e., are more likely to qualify for breast conservation therapy) and have equivalent survival to patients undergoing adjuvant chemotherapy [2,3].

With more breast cancer patients receiving NAC as a component of therapeutic management, the need for noninvasive assessment of treatment response has emerged as an important challenge for imaging. Because NAC is typically given in multiple cycles over several weeks, the ability to identify patients early in treatment who are not responding to a particular chemotherapy would allow the treating oncologist to discontinue an ineffective treatment (with potential short-term and long-term toxicities) and substitute an alternative regimen. Additionally, since pathological response is correlated with disease-free and overall survival [4,5], early noninvasive response assessment may have similar prognostic significance [6].

Prospective comparisons of different noninvasive imaging modalities have identified magnetic resonance imaging (MRI) as a useful technique in the setting of NAC for breast cancer [7,8]. Among different MRI approaches, dynamic contrast enhanced MRI (DCE-MRI) is considered especially promising due to its ability to assess changes in tumor vascularity in addition to changes in gross tumor size. To the extent that gross tumor shrinkage may lag behind changes in tumor vascularity in the context of a biological treatment response, DCE-MRI may be able to predict response earlier than techniques oriented exclusively toward tumor size.

DCE-MRI is an umbrella term used to describe a spectrum of MRI techniques and analytic approaches including both quantitative and semi-quantitative methods applied to data acquired via high and low temporal resolution sampling [9]. The literature on DCE-MRI for assessment of breast cancer response to NAC has evolved along two main avenues of investigation: fully quantitative approaches using different tracer pharmacokinetic models applied to high temporal resolution acquisitions [10–14], and a variety of alternative approaches employing semi-quantitative analyses of low temporal resolution/high spatial resolution images [15–18]. Both approaches have their strengths: theoretical considerations and empirical data suggest that diagnostic performance of DCE-MRI may improve with increasing temporal resolution [19], but semi-quantitative approaches may offer greater reproducibility by virtue of their simplicity, especially when deployed across multiple sites in a large-scale clinical trial [20].

Given the relative advantages of these two approaches, and out of consideration that a blended approach might offer enhanced reproducibility while retaining the ability to characterize changes in tumor vascularity with precision, we undertook this study to

investigate whether a semi-quantitative analysis of high temporal resolution DCE-MRI data could provide useful early information regarding breast cancer response to NAC. We employed a semi-quantitative approach for kinetic curve type categorization similar to one previously applied by other investigators for initial characterization of lesions as benign or malignant [21]. While others have studied changes in tumor washout kinetics during preoperative therapy [15], this is the first attempt to our knowledge to evaluate whether a semi-quantitative analysis of high temporal resolution DCE-MRI data can be used to predict pathological response after one cycle of NAC.

2. Materials and methods

2.1. Patients and clinical protocol

Patients with pathologically proven LABC who were scheduled to receive NAC were eligible for this IRB-approved prospective study. After providing informed consent, patients underwent DCEMRI before and after one cycle of NAC. Human epidermal growth factors 2 (HER2) positive patients received paclitaxel, carboplatin, and trastuzumab every three weeks for six cycles. Most patients with HER2 negative tumors received doxorubicin and cyclophosphamide administered every two weeks for four cycles followed by twelve weekly cycles of paclitaxel, although a subset of patients with “triple negative” disease (i.e., negative for estrogen receptor (ER), progesterone receptor (PR), and HER2 overexpression) received weekly cisplatin and paclitaxel combined with either everolimus or placebo for twelve weeks as part of a separate clinical trial. After NAC, patients underwent either mastectomy or breast conservation therapy.

2.2. Pathological analysis

After surgery, specimens were evaluated for pathological treatment response. A patient was classified as having had a pathological complete response (pCR) to NAC if she had complete absence of residual disease at the primary tumor site and complete absence of disease in any resected lymph nodes. A patient was considered as not having achieved a pCR if she had any residual disease at the primary tumor site and/or residual lymph node disease.

2.3. MRI methods

Patients were screened prior to imaging to ensure adequate renal function before administration of intravenous gadolinium contrast. The study protocol specified a minimum estimated glomerular filtration rate (eGFR) of 90 mL/min, with this value obtained within 30 days of imaging.

MRI was performed on a Philips 3 T Achieva MR scanner (Philips Healthcare, Best, The Netherlands) using a 4-channel receive double-breast coil (Invivo Inc., Gainesville, FL). High temporal resolution DCE-MRI data were acquired using an RF-spoiled 3D gradient echo multi-flip angle acquisition with TR = 7.9 ms, TE = 4.6 ms, a flip angle of 20°, one signal acquisition, and a sensitivity encoding (i.e., SENSE) factor of 2 applied in the anterior–posterior direction. Twenty sagittal slices were acquired with a slice thickness of 5 mm, in-plane field of view (FOV) of 22 cm^2, acquisition matrix of 192 × 192, and no interslice spacing. Dynamic scanning was performed over 25 acquisitions with a temporal resolution of 16 s per acquisition, for a total scan time of 400 s. The first three acquisitions were unenhanced baseline scans; after the third baseline scan, 0.1 mmol/kg (9–15 mL) of gadopentetate dimeglumine (Gd-DTPA, Magnevist, Wayne, NJ) was administered through an antecubital vein catheter via a power injector (Medrad, Inc., Warrendale, PA) at 2 mL/s, followed by a saline flush. An investigator with over 10 years of experience in medical

image registration (X.L.) monitored cine loops of the dynamic frames to ensure that images were not corrupted by patient motion.

2.4. Image analysis

Graphical user interface (GUI) software was constructed using Matlab 2010a (MathWorks, Natick, MA) to display acquired images and to facilitate data extraction (Fig. 1). Using the GUI software, two board-certified radiologists (R.A. and T.H.), each with more than five years of breast MRI experience, measured all lesions and drew regions of interest (ROIs) around lesion volumes on the pretreatment and post-cycle 1 image sets.

Data extracted for analysis included lesion size, perceived enhancement, and semi-quantitative enhancement kinetics parameters. For lesion size, tumor measurements were made in long-axis and short-axis using the slice on which the lesion appeared largest. Following the methodology described by Loo et al. [17], measurements were performed both during the initial phase of enhancement (before 120 s) and during the late phase of enhancement (at 400 s).

For perceived enhancement, each radiologist performed a subjective assessment of the percentage of lesion volume demonstrating enhancement at each timepoint. Enhancement was graded in quartiles as follows: less than 25% enhancement, 25% to 50% enhancement, 50% to 75% enhancement, and greater than 75% enhancement.

For semi-quantitative analysis of enhancement kinetics, the GUI first filtered for voxels within each ROI demonstrating signal intensity increases of either ≥50% or ≥100% over baseline following contrast administration, thus removing any nonenhancing voxels or voxels with low-level enhancement. Then, using the ≥50% and ≥100% enhancement filters, the GUI automatically calculated the percentage of voxels within each ROI exhibiting progressive (Type I), plateau (Type II), or washout (Type III) enhancement kinetics [22]. Enhancement type for each voxel was designated with reference to SI_{slope} for that voxel, defined as

$$SI_{slope} = [(SI_{\text{tail}} - SI_{\text{peak}}) / SI_{\text{peak}}] \times 100\%$$

where SI_{peak} was the peak signal intensity during the first 120 s following contrast injection and SI_{tail} was the average signal intensity over the final two dynamic acquisitions. Voxels were designated as having progressive (Type I) enhancement kinetics if SI_{slope} was +10% or greater, plateau (Type II) if SI_{slope} was between −10% and +10%, and washout (Type III) if SI_{slope} was −10% or less. In order to minimize anomalies from spurious signal intensity fluctuations over the course of a dynamic contrast run, the entire time–signal intensity curve for each voxel was smoothed by a moving average filter of length three before entering into the enhancement kinetics analysis.

2.5. Statistical analysis

A non-parametric Spearman rank correlation analysis was used to estimate the correlation between the two radiologists with respect to observed imaging parameters. Logistic regression analysis was then performed in two steps. First, as a preliminary step to select covariates, a Mann–Whitney U test was employed to examine the median difference of continuous variables (e.g., size measurements) between pathological responders and non-responders, and a Fisher's exact test was used to determine the association between categorical variables (e.g., perceived enhancement) and pathological response or non-response. For variables found to discriminate patients with a pCR at a p-value of less than or equal to 0.05, receiver operating characteristic (ROC) analysis was then performed using a

logistic regression model. 95% confidence intervals for the area under the curve (AUC) were generated based on 2000 bootstrap samples. All data were analyzed using publicly available R version 2.11.0 statistical software.

3. Results

3.1. Patient characteristics and pathological response

A total of 21 patients completed the study. Table 1 presents an overview of patient and tumor characteristics. Patients underwent post-cycle 1 scanning at a median of 14 days following baseline imaging (range: 7–28 days). At pathological analysis, 9 patients were classified as having achieved a pCR. Table 2 provides a summary of tumor type, scan timing, and pathological response for all patients.

3.2. Interobserver variability

The non-parametric Spearman rank correlation analysis demonstrated statistically significant correlation between both radiologists for all continuous variable measurements with exception of short-axis lesion diameter during initial phase of enhancement (ρ for short-axis lesion diameter during initial phase of enhancement = 0.33, $p = 0.14$; mean ρ for all other measurements = 0.77, median = 0.75, $p = 0.00–0.02$). The correlation between the two radiologists was deemed sufficient to allow observations from both radiologists to be averaged together for all subsequent analyses.

3.3. Imaging parameter measurements and predictive ability

3.3.1. Pretreatment parameters—No pretreatment imaging parameters were able to discriminate patients with an eventual pCR ($p = 0.22–1.00$) (Table 3).

3.3.2. Percentage change in parameters after first cycle of chemotherapy—Change in percentage of voxels demonstrating washout kinetics with a ≥100% enhancement threshold filter discriminated patients with an eventual pCR ($p = 0.04$) (Table 4). ROC analysis for this variable yielded an AUC of 0.77 (95% confidence interval, [0.53, 0.96]) (Fig. 2). Accuracy was maximized at a cutoff of 64% decrease from baseline in percentage of voxels demonstrating washout kinetics; at this value, sensitivity was 100% and specificity was 66.67% for predicting pCR.

No other parameter change demonstrated statistically significant predictive ability, although percentage change in long axis diameter measured early in enhancement did approach statistical significance ($p = 0.08$). Fig. 3 summarizes all of the parameter change data.

4. Discussion

In recent years, an extensive literature has emerged around advanced imaging techniques for the prediction of breast cancer response to NAC. Techniques currently under investigation include volumetric ultrasonography, positron emission tomography, and magnetic resonance imaging comprising both conventional anatomic and advanced functional imaging methods [23–35]. This is an important area of investigation because current trials are investigating the use of different NAC regimens in multiple patients groups, including patients with smaller tumors that are less amenable to reliable evaluation by palpation. An imaging technique with the ability to predict pathological response early in treatment could have important ramifications for patient care, including allowing the treating oncologist to discontinue an ineffective treatment and substitute an alternative regimen [36].

The literature around DCE-MRI in this setting is especially rich and varied. Investigations into DCE-MRI for the prediction of breast cancer response to NAC have employed different DCE-MRI temporal resolutions, data analysis methods, imaging timing relative to NAC, and outcome variables. In general, the literature segregates into two broad categories: studies employing fully quantitative analysis of high temporal resolution DCE-MRI data using complex pharmacodynamic modeling [10–14,37,38], and studies employing a variety of semi-quantitative analyses of low temporal resolution data [15–18]. The variation in approaches reflects the challenges of DCE-MRI protocol design in the breast, where there are competing imperatives for high spatial-resolution imaging (to depict lesion morphology and to maximize sensitivity for small disease foci) and high temporal-resolution imaging (to model subtle changes in vascular flow and permeability). It also reflects a possible disconnection between highly specialized centers, which may possess the expertise and dedicated analytic resources to perform rigorous and complex pharmacokinetic modeling, and nonspecialized clinical sites, which may have access to such techniques only through commercially available computer assisted detection (CAD) software. At the present time, it is not clear how DCE-MRI should evolve and be translated into broad clinical use for assessing breast cancer response to NAC. Advocates of quantitative analysis of high temporal resolution data might highlight promising data from pharmacokinetic modeling as well as studies suggesting increasing diagnostic performance of DCE-MRI with increasing temporal resolution [19]. Conversely, proponents of semiquantitative approaches might point to the complexity of pharmacokinetic modeling as potentially problematic, especially when trying to standardize image acquisition and analysis across multiple sites in a large-scale clinical trial; for example, a simple, semi-quantitative, three-point signal enhancement ratio (SER) approach [16,39] was chosen over more complex methods for use in the multi-site American College of Radiology Imaging Network (ACRIN) 6657/Investigation of Serial Studies to Predict Your Therapeutic Response with Imaging And moLecular Analysis (I-SPY) trial [20].

This study was performed out of consideration that a blended technique, employing a semi-quantitative analysis of high temporal resolution DCE-MRI data, might offer useful early information on breast cancer response to NAC. We adapted a straightforward method used previously by other investigators [21] to categorize individual voxels as having progressive (Type I), plateau (Type II), or washout (Type III) enhancement kinetic curves, and we found that after a single cycle of NAC, a reduction in the percentage of voxels demonstrating washout (Type III) kinetics with a ≥100% enhancement filter was significantly associated with pCR. Our AUC of 0.77 for this single predictor variable compares favorably with the AUC of 0.73 found in the ACRIN/I-SPY trial for a four-predictor variable model [20]. Other imaging parameters in our study, including lesion size measurement and subjective assessment of lesion enhancement, did not discriminate between pathological responders and non-responders.

Fig. 1 illustrates imaging results for a patient who achieved a pCR. In this example, there was a subjectively appreciable decrease after one cycle of NAC in the proportion of intralesional voxels exhibiting washout kinetics (coded red), although the lesion itself had not changed significantly in size. At the completion of NAC, however, the lesion had disappeared. The findings suggest that in this patient, a biological treatment response manifested as a change in tumor vascularity that was detectable earlier than a change in gross tumor size.

There are a number of potential advantages to our approach. First, the technique is simple and requires significantly less effort, resources, and expertise than a formal quantitative analysis. Traditional quantitative DCE-MRI analysis typically requires a pre-contrast T1 map, accurate estimation of the arterial input function (i.e., the time rate of change of the

concentration of contrast agent in a feeding artery), and pharmacokinetic modeling; none of those data or analyses was employed to arrive at the results presented here. Second, by virtue of its simplicity, this method may be more robust to variations in scanner settings, platforms, and imaging protocols, especially when deployed across multiple sites in a large-scale clinical trial, although this would have to be proved systematically. Third, a voxelwise analysis may offer the advantage of improved depiction of tumoral heterogeneity when compared to some other semiquantitative approaches that average parameter values across an entire lesion ROI.

We emphasize that this is a preliminary study with several limitations owing to our small sample size. First, our study population was heterogeneous, including patients with different breast tumor subtypes and different treatment regimens that also affected scan timing; our sample size was not large enough to perform subanalyses on response prediction performance within these subgroups. Second, our study was not powered to allow for comparison of our semi-quantitative technique against a fully quantitative pharmacodynamic modeling analysis, and we therefore make no claim that one technique is superior to the other. Third, although reduction in the percentage of voxels demonstrating washout kinetics was able to discriminate patients with pCR from patients without pCR, there remained some overlap between the two groups; indeed, we note that the greatest percentage decrease in intralesional washout voxels was observed in a patient who did not achieve a pCR (Fig. 3), a finding that will require an explanation before this approach can be considered ready for clinical translation. We anticipate the results of the present study being most useful for motivating other investigators to conduct retrospective analysis of similar datasets and for guiding future studies.

In conclusion, we have shown that semi-quantitative analysis of enhancement kinetics data from a high temporal resolution DCEMRI acquisition can predict pathological response of LABC after one cycle of NAC. Our results demonstrate the feasibility of incorporating a relatively simple semi-quantitative DCE-MRI analysis for early response assessment in settings that lack the expertise and resources for dedicated, formal quantitative analysis. These results suggest that important early treatment response information can be obtained from high temporal resolution DCE-MRI without the use of rigorous pharmacokinetic modeling.

Acknowledgments

We thank John Huff, M.D., and Yu Shyr, Ph.D., for their invaluable insights and guidance. We also thank Donna Butler, Leslie McIntosh, and Sandeep Bhave for their expert technical assistance. This project was supported by the following research grants from the National Institutes of Health (NIH): NCI 1R01CA129961, NCI 1P50 098131, NIH P30 CA68485, and NCI 1U01CA142565. We thank the Kleberg Foundation for generous support of the molecular imaging program at our Institution.

References

[1]. Kaufmann M, von Minckwitz G, Bear HD, et al. Recommendations from an international expert panel on the use of neoadjuvant (primary) systemic treatment of operable breast cancer: new perspectives 2006. Ann Oncol. 2007; 18:1927–34. [PubMed: 17998286]

[2]. Mauri D, Pavlidis N, Ioannidis JP. Neoadjuvant versus adjuvant systemic treatment in breast cancer: a meta-analysis. J Natl Cancer Inst. 2005; 97:188–94. [PubMed: 15687361]

[3]. Fisher B, Bryant J, Wolmark N, et al. Effect of preoperative chemotherapy on the outcome of women with operable breast cancer. J Clin Oncol. 1998; 16:2672–85. [PubMed: 9704717]

[4]. Chollet P, Amat S, Cure H, et al. Prognostic significance of a complete pathological response after induction chemotherapy in operable breast cancer. Br J Cancer. 2002; 86:1041–6. [PubMed: 11953845]

[5]. Wolff AC, Berry D, Carey LA, et al. Research issues affecting preoperative systemic therapy for operable breast cancer. J Clin Oncol. 2008; 26:806–13. [PubMed: 18258990]

[6]. Li SP, Makris A, Beresford MJ, et al. Use of dynamic contrast-enhanced MR imaging to predict survival in patients with primary breast cancer undergoing neoadjuvant chemotherapy. Radiology. 2011; 260:68–78. [PubMed: 21502383]

[7]. Londero V, Bazzocchi M, Del Frate C, et al. Locally advanced breast cancer: comparison of mammography, sonography and MR imaging in evaluation of residual disease in women receiving neoadjuvant chemotherapy. Eur Radiol. 2004; 14:1371–9. [PubMed: 14986052]

[8]. Yeh E, Slanetz P, Kopans DB, et al. Prospective comparison of mammography, sonography, and MRI in patients undergoing neoadjuvant chemotherapy for palpable breast cancer. AJR Am J Roentgenol. 2005; 184:868–77. [PubMed: 15728611]

[9]. Yankeelov TE, Gore JC. Dynamic contrast enhanced magnetic resonance imaging in oncology: theory, data acquisition, analysis, and examples. Curr Med Imaging Rev. 2009; 3:91–107. [PubMed: 19829742]

[10]. Ah-See ML, Makris A, Taylor NJ, et al. Early changes in functional dynamic magnetic resonance imaging predict for pathologic response to neoadjuvant chemotherapy in primary breast cancer. Clin Cancer Res. 2008; 14:6580–9. [PubMed: 18927299]

[11]. Manton DJ, Chaturvedi A, Hubbard A, et al. Neoadjuvant chemotherapy in breast cancer: early response prediction with quantitative MR imaging and spectroscopy. Br J Cancer. 2006; 94:427–35. [PubMed: 16465174]

[12]. Padhani AR, Hayes C, Assersohn L, et al. Prediction of clinicopathologic response of breast cancer to primary chemotherapy at contrast-enhanced MR imaging: initial clinical results. Radiology. 2006; 239:361–74. [PubMed: 16543585]

[13]. Pickles MD, Lowry M, Manton DJ, Gibbs P, Turnbull LW. Role of dynamic contrast enhanced MRI in monitoring early response of locally advanced breast cancer to neoadjuvant chemotherapy. Breast Cancer Res Treat. 2005; 91:1–10. [PubMed: 15868426]

[14]. Wasser K, Klein SK, Fink C, et al. Evaluation of neoadjuvant chemotherapeutic response of breast cancer using dynamic MRI with high temporal resolution. Eur Radiol. 2003; 13:80–7. [PubMed: 12541113]

[15]. El Khoury C, Servois V, Thibault F, et al. MR quantification of the washout changes in breast tumors under preoperative chemotherapy: feasibility and preliminary results. AJR Am J Roentgenol. 2005; 184:1499–504. [PubMed: 15855104]

[16]. Hylton N. Dynamic contrast-enhanced magnetic resonance imaging as an imaging biomarker. J Clin Oncol. 2006; 24:3293–8. [PubMed: 16829653]

[17]. Loo CE, Teertstra HJ, Rodenhuis S, et al. Dynamic contrast-enhanced MRI for prediction of breast cancer response to neoadjuvant chemotherapy: initial results. AJR Am J Roentgenol. 2008; 191:1331–8. [PubMed: 18941065]

[18]. Martincich L, Montemurro F, De Rosa G, et al. Monitoring response to primary chemotherapy in breast cancer using dynamic contrast-enhanced magnetic resonance imaging. Breast Cancer Res Treat. 2004; 83:67–76. [PubMed: 14997056]

[19]. El Khouli RH, Macura KJ, Barker PB, Habba MR, Jacobs MA, Bluemke DA. Relationship of temporal resolution to diagnostic performance for dynamic contrast enhanced MRI of the breast. J Magn Reson Imaging: JMRI. 2009; 30:999–1004.

[20]. Hylton NM, Blume JD, Bernreuter WK, et al. Locally advanced breast cancer: MR imaging for prediction of response to neoadjuvant chemotherapy—results from ACRIN 6657/I-SPY Trial. Radiology. 2012; 263:663–72. [PubMed: 22623692]

[21]. El Khouli RH, Macura KJ, Jacobs MA, et al. Dynamic contrast-enhanced MRI of the breast: quantitative method for kinetic curve type assessment. AJR Am J Roentgenol. 2009; 193:W295–300. [PubMed: 19770298]

[22]. Macura KJ, Ouwerkerk R, Jacobs MA, Bluemke DA. Patterns of enhancement on breast MR images: interpretation and imaging pitfalls. Radiographics. 2006; 26:1719–34. [PubMed: 17102046]

[23]. Baek HM, Chen JH, Nie K, et al. Predicting pathologic response to neoadjuvant chemotherapy in breast cancer by using MR imaging and quantitative 1H MR spectroscopy. Radiology. 2009; 251:653–62. [PubMed: 19276320]

[24]. Chen X, Moore MO, Lehman CD, et al. Combined use of MRI and PET to monitor response and assess residual disease for locally advanced breast cancer treated with neoadjuvant chemotherapy. Acad Radiol. 2004; 11:1115–24. [PubMed: 15530804]

[25]. Gounaris I, Provenzano E, Vallier AL, et al. Accuracy of unidimensional and volumetric ultrasound measurements in predicting good pathological response to neoadjuvant chemotherapy in breast cancer patients. Breast Cancer Res Treat. 2011; 127:459–69. [PubMed: 21437610]

[26]. Jacobs MA, Ouwerkerk R, Wolff AC, et al. Monitoring of neoadjuvant chemotherapy using multiparametric, (2)(3)Na sodium MR, and multimodality (PET/CT/MRI) imaging in locally advanced breast cancer. Breast Cancer Res Treat. 2011; 128:119–26. [PubMed: 21455671]

[27]. Jacobs MA, Stearns V, Wolff AC, et al. Multiparametric magnetic resonance imaging, spectroscopy and multinuclear ((2)(3)Na) imaging monitoring of preoperative chemotherapy for locally advanced breast cancer. Acad Radiol. 2010; 17:1477–85. [PubMed: 20863721]

[28]. Keam B, Im SA, Koh Y, et al. Early metabolic response using FDG PET/CT and molecular phenotypes of breast cancer treated with neoadjuvant chemotherapy. BMC Cancer. 2011; 11:452. [PubMed: 22011459]

[29]. Kolesnikov-Gauthier H, Vanlemmens L, Baranzelli MC, et al. Predictive value of neoadjuvant chemotherapy failure in breast cancer using FDG-PET after the first course. Breast Cancer Res Treat. 2012; 131:517–25. [PubMed: 22037787]

[30]. Meisamy S, Bolan PJ, Baker EH, et al. Neoadjuvant chemotherapy of locally advanced breast cancer: predicting response with in vivo (1)H MR spectroscopy—a pilot study at 4 T. Radiology. 2004; 233:424–31. [PubMed: 15516615]

[31]. Park SH, Moon WK, Cho N, et al. Diffusion-weighted MR imaging: pretreatment prediction of response to neoadjuvant chemotherapy in patients with breast cancer. Radiology. 2010; 257:56–63. [PubMed: 20851939]

[32]. Partridge SC, Gibbs JE, Lu Y, Esserman LJ, Sudilovsky D, Hylton NM. Accuracy of MR imaging for revealing residual breast cancer in patients who have undergone neoadjuvant chemotherapy. AJR Am J Roentgenol. 2002; 179:1193–9. [PubMed: 12388497]

[33]. Partridge SC, Gibbs JE, Lu Y, et al. MRI measurements of breast tumor volume predict response to neoadjuvant chemotherapy and recurrence-free survival. AJR Am J Roentgenol. 2005; 184:1774–81. [PubMed: 15908529]

[34]. Sharma U, Danishad KK, Seenu V, Jagannathan NR. Longitudinal study of the assessment by MRI and diffusion-weighted imaging of tumor response in patients with locally advanced breast cancer undergoing neoadjuvant chemotherapy. NMR Biomed. 2009; 22:104–13. [PubMed: 18384182]

[35]. Tateishi U, Miyake M, Nagaoka T, et al. Neoadjuvant chemotherapy in breast cancer: prediction of pathologic response with PET/CT and dynamic contrast-enhanced MR imaging—prospective assessment. Radiology. 2012; 263:53–63. [PubMed: 22438441]

[36]. Abramson RG, Arlinghaus LR, Weis JA, et al. Current and emerging quantitative magnetic resonance imaging methods for assessing and predicting the response of breast cancer to neoadjuvant therapy. Breast cancer: targets and therapy. 2012; 2012:139–54.

[37]. Yu HJ, Chen JH, Mehta RS, Nalcioglu O, Su MY. MRI measurements of tumor size and pharmacokinetic parameters as early predictors of response in breast cancer patients undergoing neoadjuvant anthracycline chemotherapy. J Magn Reson Imaging. 2007; 26:615–23. [PubMed: 17729334]

[38]. Yu Y, Jiang Q, Miao Y, et al. Quantitative analysis of clinical dynamic contrast-enhanced MR imaging for evaluating treatment response in human breast cancer. Radiology. 2010; 257:47–55. [PubMed: 20713609]

[39]. Li KL, Partridge SC, Joe BN, et al. Invasive breast cancer: predicting disease recurrence by using high-spatial-resolution signal enhancement ratio imaging. Radiology. 2008; 248:79–87. [PubMed: 18566170]

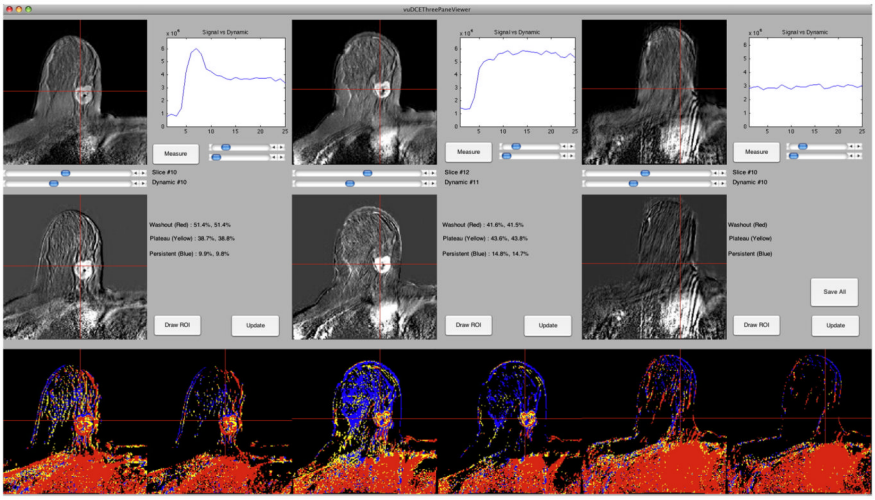

Fig. 1.

Screen capture from the graphical user interface (GUI). The top row displays postcontrast MRI images from all three timepoints (baseline, after one cycle of NAC, and at completion of NAC). The graphs depict time–signal intensity curves for single voxels, chosen by the user by placing cross-hairs within the images. The middle row displays subtraction images corresponding to the slices in the top row. The bottom row contains parametric color maps representing the shape of the enhancement curve for each voxel within the slice, with one map using a 50% enhancement filter and the other map using a 100% enhancement filter. Blue = progressive (type I) kinetics, yellow = plateau (type II) kinetics, red = washout (type III) kinetics.

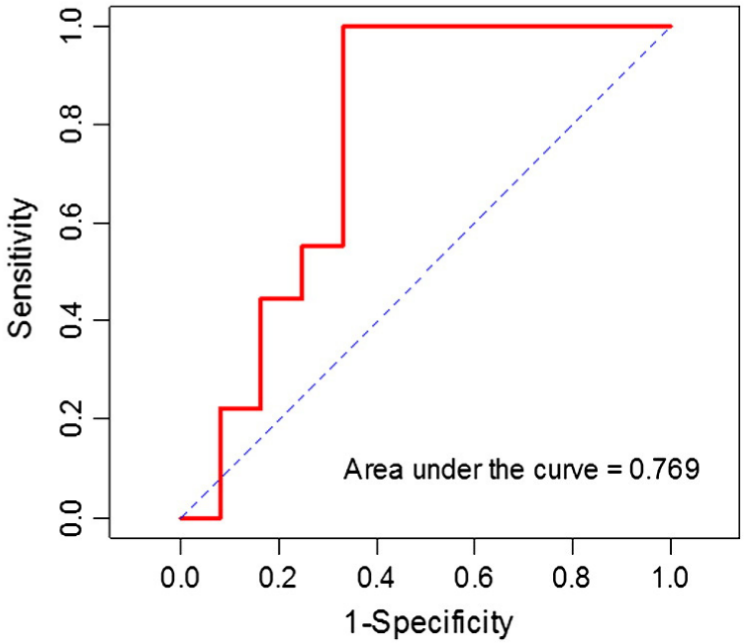

Fig. 2.
Receiver operator characteristic (ROC) analysis for percentage change in voxels demonstrating washout kinetics with a 100% enhancement filter.

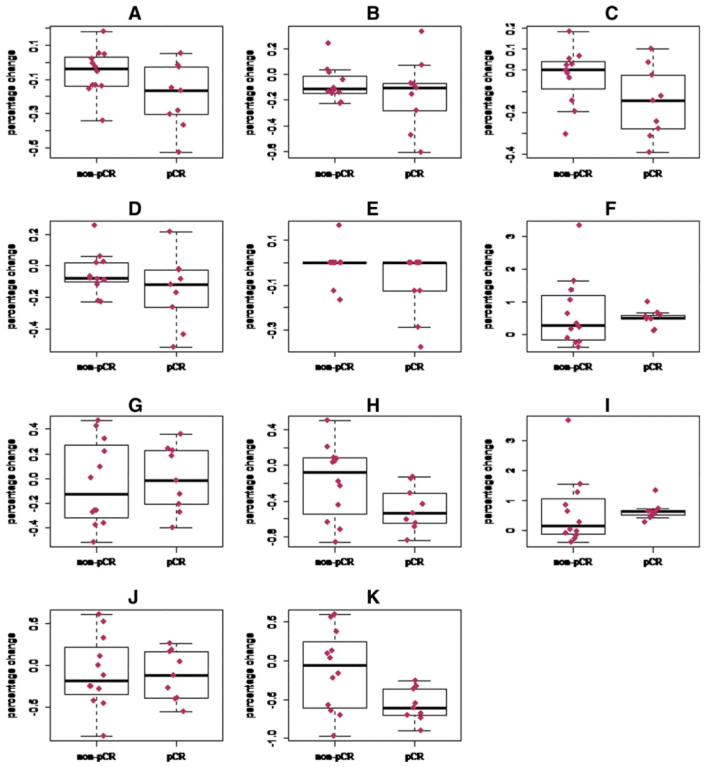

Fig 3.

Box plots illustrating percentage changes from baseline to post-cycle 1 for all imaging parameters, stratified by pathological response. (A) Lesion size, long axis, early in enhancement. (B) Lesion size, short axis, early in enhancement. (C) Lesion size, long axis, late in enhancement. (D) Lesions size, short axis, late in enhancement. (E) Radiologists' subjective assessment of lesion enhancement, graded in quartiles (see text). (F) Percentage of voxels exhibiting progressive (Type I) enhancement kinetics with a ≥50% enhancement filter. (G) Percentage of voxels exhibiting plateau (Type II) kinetics with a ≥50% enhancement filter. (H) Percentage of voxels exhibiting washout (Type III) kinetics with a ≥50% enhancement filter. (I) Percentage of voxels exhibiting progressive (Type I) kinetics with a ≥100% enhancement filter. (J) Percentage of voxels exhibiting plateau (Type II) kinetics with a ≥100% enhancement filter. (K) Percentage of voxels exhibiting washout (Type III) kinetics with a ≥100% enhancement filter. pCR = pathological complete response.

Table 1

Patient and tumor characteristics.

Variable	Value
Number of patients	21
Patient age (years)	
Mean	45
Range	28–60
Baseline tumor diameter, clinical (cm)	
Mean	5.6
Range	2–12
Immunostaining	
ER+ and/or PR+	7
HER2+ (including ER+ and ER−)	7
Triple negative	7
Tumor grade	
Low	3
Intermediate	6
High	12
Surgery	
Mastectomy	10
Breast conservation therapy	11

ER = estrogen receptor. HER2 = human epidermal growth factor receptor 2 (ErbB2). PR = progesterone receptor. “Triple negative” = ER−/PR−/HER2−.

Table 2

Patient tumor type, timing of “post-cycle 1” scan, and pathological response.

Patient number	Tumor type	Timing of “post-cycle 1” scan (days after baseline scan)	Pathological response
01	HER2 +	21	pCR
02	HER2 +	7	pCR
03	ER+ and/or PR+	14	non-pCR
04	ER+ and/or PR+	13	pCR
05	Triple negative	17	non-pCR
06	HER2 +	24	pCR
07	ER+ and/or PR+	14	non-pCR
08	HER2 +	18	non-pCR
09	ER+ and/or PR+	17	non-pCR
10	HER2 +	13	non-pCR
11	Triple negative	15	pCR
12	ER+ and/or PR+	14	non-pCR
13	HER2 +	25	non-pCR
14	HER2 +	14	pCR
15	Triple negative	16	pCR
16	ER+ and/or PR+	28	non-pCR
17	Triple negative	7	non-pCR
18	Triple negative	9	non-pCR
19	ER+ and/or PR+	13	pCR
20	Triple negative	15	pCR
21	Triple negative	9	non-pCR

ER = estrogen receptor. HER2 = human epidermal growth factor receptor 2 (ErbB2). PR = progesterone receptor. “Triple negative” = ER−/PR−/HER2−.

Table 3

Analysis of pretreatment imaging parameters for discriminating pCR.

Imaging parameter	Values for patients with a pCR		Values for patients without a pCR		p-value for discriminating patients with a pCR
	Median	Range	Median	Range	
Lesion size (mm)					
LAD (early: before 120 s)	26.8	15.9 to 74.8	35.2	12.5 to 54.4	.70
SAD (early: before 120 s)	17.7	13.4 to 32.6	14.0	9.4 to 34.3	.27
LAD (late: 400 s)	27.3	14.4 to 75.7	35.3	13.5 to 55.2	.75
SAD (late: 400 s)	19.6	13.6 to 36.0	13.8	9.8 to 34.7	.22
Enhancement	4	3 to 4	3.5	2.5 to 4	.51
Kinetics					
50% threshold					
% washout	34.7	5.7 to 47.2	22.2	5.1 to 63.5	.86
% plateau	36.1	29.6 to 46.2	34.0	28.5 to 56.5	.75
% progressive	32.2	17.4 to 55.1	34.6	8.0 to 64.8	1.00
100% threshold					
% washout	35.8	6.1 to 47.2	16.4	5.5 to 48.4	.60
% plateau	36.2	30.0 to 46.7	35.5	16.2 to 55.5	.92
% progressive	31.3	16.7 to 48.6	41.5	9.3 to 78.3	.81

pCR = pathological complete response, LAD = long-axis diameter, SAD = short-axis diameter.

Table 4

Analysis of imaging parameter changes (from pretreatment to after cycle 1) for discriminating pCR.

Imaging parameter	% change for patients with a pCR		% change for patients without a pCR		p-value for discriminating patients with a pCR
	Median	Range	Median	Range	
Lesion size (mm)					
LAD (early)	−17	−53 to +6	−4	−34 to +18	.08
SAD (early)	−11	−61 to +33	−12	−23 to +24	.70
LAD (late)	−15	−39 to +10	0	−30 to +18	.11
SAD (late)	−12	−52 to +22	−8	−23 to +26	.25
Enhancement	0	−38 to 0	0	−17 to +17	.49
Kinetics					
50% threshold					
% progressive (Type I)	+ 49	+ 11 to +99	+ 28	−39 to+335	.75
% plateau (Type II)	−2	−39 to +36	−13	−51 to +47	.81
% washout (Type III)	−54	−84 to −12	−8	−86 to +50	.11
100% threshold					
% progressive (Type I)	+ 62	+26to + 134	+16	−40 to +336	.35
% plateau (Type II)	−12	−56 to +26	−19	−86 to +61	.92
% washout (Type III)	**−62**	**−90 to −26**	**−7**	**−97 to + 58**	**.04**

Bold = statistically significant at $p < .05$. pCR = pathological complete response, LAD = long-axis diameter, SAD = short-axis diameter, − = percentage decrease, + = percentage increase.